

# Layered Image Vectorization via Semantic Simplification

ZHENYU WANG, Shenzhen University, China  
 JIANXI HUANG, Shenzhen University, China  
 ZHIDA SUN, Shenzhen University, China  
 DANIEL COHEN-OR, Tel-Aviv University, Isreal  
 MIN LU\*, Shenzhen University, China

This work presents a novel progressive image vectorization technique aimed at generating layered vectors that represent the original image from coarse to fine detail levels. Our approach introduces semantic simplification, which combines Score Distillation Sampling and semantic segmentation to iteratively simplify the input image. Subsequently, our method optimizes the vector layers for each of the progressively simplified images. Our method provides robust optimization, which avoids local minima and enables adjustable detail levels in the final output. The layered, compact vector representation enhances usability for further editing and modification. Comparative analysis with conventional vectorization methods demonstrates our technique's superiority in producing vectors with high visual fidelity, and more importantly, maintaining vector compactness and manageability. The project homepage is [https://szuviz.github.io/layered\\_vectorization/](https://szuviz.github.io/layered_vectorization/).

CCS Concepts: • **Computing methodologies** → **Shape inference**.

Additional Key Words and Phrases: Vectorization; Image Simplification; Layered Vector Representation; SVG

## ACM Reference Format:

Zhenyu Wang, Jianxi Huang, Zhida Sun, Daniel Cohen-Or, and Min Lu. 2024. Layered Image Vectorization via Semantic Simplification. 1, 1 (June 2024), 11 pages. <https://doi.org/10.1145/nnnnnnn.nnnnnnn>

## 1 INTRODUCTION

Vector graphics represent images at the object level rather than the pixel level, resulting in simplified, textureless representations that are more symbolic than realistic [Ferraiolo et al. 2000]. Such vectorized representations use simple geometric primitives like lines, curves, and shapes, enabling vectors to scale and resize without quality loss. The efficiency of vectors in storing and transmitting complex visual content with minimal data makes it popular for easy editing and seamless integration of various elements. These vectorized representations are commonly encoded in Scalable Vector Graphics (SVG) format. Creating effective SVG representations often demands considerable artistic effort. State-of-the-art vectorization methods produce complex outputs that compromise usability and

\*Corresponding Author

Authors' addresses: Zhenyu Wang, [trovato@corporation.com](mailto:trovato@corporation.com), Shenzhen University, China; Jianxi Huang, [kinhei927@gmail.com](mailto:kinhei927@gmail.com), Shenzhen University, China; Zhida Sun, [zhdsun@gmail.com](mailto:zhdsun@gmail.com), Shenzhen University, China; Daniel Cohen-Or, [cohenor@gmail.com](mailto:cohenor@gmail.com), Tel-Aviv University, Isreal; Min Lu, [lumin.vis@gmail.com](mailto:lumin.vis@gmail.com), Shenzhen University, China.

Permission to make digital or hard copies of all or part of this work for personal or classroom use is granted without fee provided that copies are not made or distributed for profit or commercial advantage and that copies bear this notice and the full citation on the first page. Copyrights for components of this work owned by others than ACM must be honored. Abstracting with credit is permitted. To copy otherwise, or republish, to post on servers or to redistribute to lists, requires prior specific permission and/or a fee. Request permissions from [permissions@acm.org](mailto:permissions@acm.org).

© 2024 Association for Computing Machinery.

XXXX-XXXX/2024/6-ART \$15.00

<https://doi.org/10.1145/nnnnnnn.nnnnnnn>

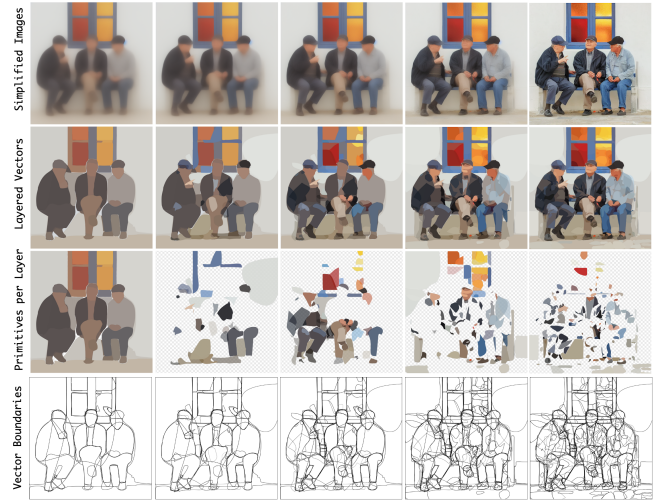


Fig. 1. Layered vectorization: by generating a sequence of semantically simplified images (top row), our technique constructs vectors with progressively finer levels of detail (second row from the top). This process generates visual primitives layer by layer (third row), keeping the primitives compactly within the boundaries of semantic groups (bottom row).

compactness [Jain et al. 2023; Ma et al. 2022]. The challenge of image vectorization into manageable representations remains significant.

In this paper, we present a novel approach to image vectorization, introducing a progressive technique that generates compact layered SVG representations. Our method constructs these layers to encapsulate coarse-to-fine details, offering a comprehensive abstraction of the original image. Key to our technique is the process of semantic simplification, which generates a series of progressively simplified versions of the input image (see the top row in Figure 1). Our image simplification technique is based on the score distillation sampling (SDS) [Poole et al. 2022] combined with a semantic segmentation (SAM) [Kirillov et al. 2023]. Corresponding SVG layers are generated, mirroring the progressive abstraction process of the image (Figure 1). By harnessing a popular differential rasterizer [Li et al. 2020], our method optimizes each SVG layer representation by back-propagating a loss function computed on the generated raster image.

Our progressive vectorization approach provides a series of layers, which, by construction, are organized in a back-to-front and coarse-to-fine manner, where the vector primitives tend to be semantically grouped. Moreover, our layered vectorization breaks a complex problem into manageable pieces and hence provides robust



Fig. 2. Five levels of detail generated with our layered image vectorization. Note that the front layers add details on top of the back layers.

optimization, effectively avoiding the pitfalls of local minima. Consequently, it tends to yield a compact representation and offers control over the degree of detail in the final vectorized image (see Figure 2). All together, these qualities result in a convenient, easy-to-handle, and user-friendly vectorized representation.

In our experiments, we compare our progressive vectorization approach with state-of-the-art methods and demonstrate its powerful abstraction capabilities. Through extensive evaluations, we highlight the effectiveness and efficiency of our method in generating compact and manageable SVG representations. Furthermore, the back-to-front layered organization is particularly user-friendly for interactive editing. Our method not only improves the vectorization process but also produces intuitive and easy-to-manipulate vectors.

## 2 RELATED WORK

### 2.1 Image Vectorization

Image vectorization transforms rasters to vector representations using geometric primitives, enabling resolution independence and editability crucial for applications like digital art and design. Existing methods for image vectorization fall into two categories, i.e., algorithm-driven and machine learning-based approaches, which have undergone recent reviews [Dziuba et al. 2023; Tian and Günther 2024].

Early work in this field focused on developing algorithms for tracing and approximating image contours using various geometric primitives, such as line segments, curves, and splines [Lecot and Levy 2006]. Classical methods for image vectorization aimed for compact vector representations matching human perception through piecewise curve fitting guided by perceptual cues [Dominici et al. 2020; Hoshyari et al. 2018], or layered color gradient region decompositions balancing reconstruction and simplicity [Du et al. 2023; Favreau et al. 2017]. Other classical vectorization methods for none object-based vector representation, such as mesh-based representations [Liao et al. 2012; Sun et al. 2007; Xia et al. 2009], curve-based representations [Xie et al. 2014], superpixel clustering [Achanta and Susstrunk 2017], are beyond this work’s scope. In this work, the focus is on the object-level vectorization approach.

In recent years, we have witnessed growing interest in learning-based approaches for image vectorization. A key enabler is the development of differentiable rasterizers (e.g., *DiffVG* [Li et al. 2020], *Differentiable Compositor* [Reddy et al. 2020]) that bridge the vector and raster domains, allowing neural networks to be trained to generate vector outputs by optimizing raster losses and constraints. Some methods focus on reconstructing general vector graphics like SVGs from raster inputs [Hirschorn et al. 2024; Ma et al. 2022], aiming for domain-agnostic compact representations through techniques like iterative Bézier path generation/optimization and shape reduction. Others target specific domains like clipart [Shen and Chen 2022] or technical drawings [Egiazarian et al. 2020], exploiting inductive biases about the input distribution. Common strategies include iterative layer/primitive synthesis, rasterizing vector outputs for loss computation, and optimizing vector parameters using metrics like shape similarity and perceptual losses.

These data-driven vectorization approaches enable flexible editing and synthesis capabilities that are challenging for traditional methods while producing representations suitable for downstream applications. Similar to *LIVE* [Ma et al. 2022], our method iteratively refines vector representations by adding and optimizing closed paths. However, our approach progressively simplifies the target image, effectively capturing its underlying layered structure with basic primitives (see Figure 1).

### 2.2 Vector Generation

The pace of advancement in content generation areas, particularly vector graphics generation, has accelerated in recent years with the advent of AI-driven approaches. Existing works present a diverse range of techniques, highlighting the growing interest and importance of this research domain. Some approaches focus on generative models that capture the statistical dependencies and richness of vector graphics datasets. For instance, *SVG-VAE* [Lopes et al. 2019] applies sequential generative models based on a font dataset, while *DeepSVG* [Carrier et al. 2020] tackles complex SVG icon generation and interpolation with a hierarchical generative network. Other methods leverage pre-trained models to generate vector graphics without requiring additional training on vector data. *CLIPDraw* [Frans et al. 2022] utilizes a pre-trained language-image model to generate vector drawings from natural language input, aligning with *VectorFusion* [Jain et al. 2023], which explores using text-conditioned diffusion models trained on raster images to generate SVG-exportable vector graphics.

Addressing the limited availability of high-quality vector graphics datasets, *Im2Vec* [Reddy et al. 2021] proposes a neural network that generates complex vector graphics from readily available raster training images using a differentiable rasterization pipeline. More recently, multimodal integration of language and vision models has also been explored. *StarVector* [Rodriguez et al. 2023] introduces a model that effectively combines Code Generation Large Language Models (CodeLLMs) and vision models, emphasizing the disentanglement of representations. We take inspiration from these works and also leverage a text-to-image diffusion model to enhance the process of progressive image simplification.

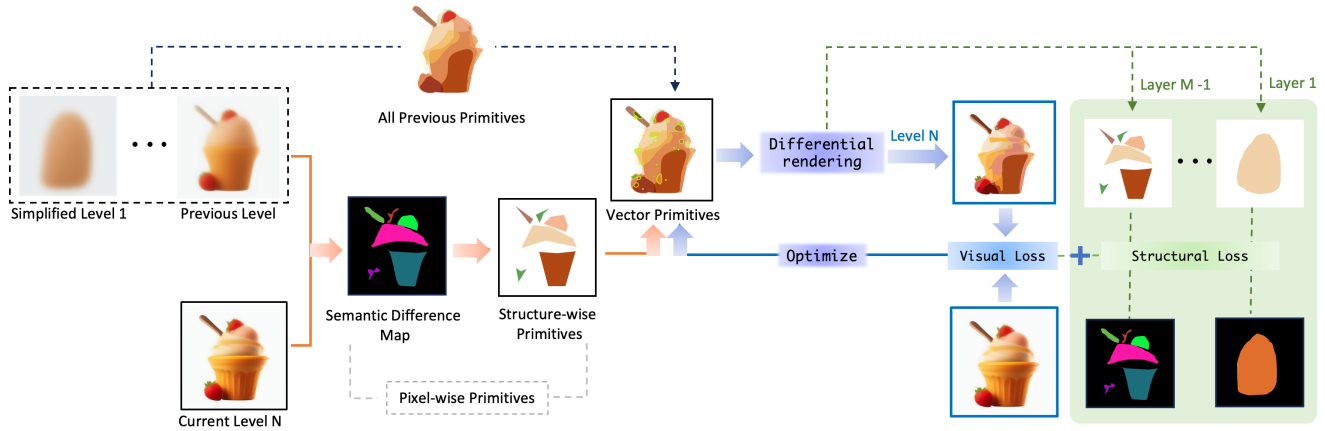


Fig. 3. Layered vectorization: to optimize the current level, primitives are initialized at regions where semantic and visual differences are most pronounced. The vector primitives are rendered and optimized by backpropagating a joint loss function, enhancing both structural representation and visual appearance.

### 2.3 Image Abstraction and Simplification

Image abstraction is a transformative process that simplifies images while preserving their essential visual characteristics. There are two main types of work in this area, i.e., sketch abstraction and geometric abstraction. In *sketch abstraction*, recent works tackle line drawing simplicity through techniques like Koley et al. [2024]’s abstraction-aware framework and approaches like *CLIPDraw* [Frans et al. 2022], *CLIPasso* [Vinker et al. 2022] and *CLIPascene* [Vinker et al. 2023] that synthesize abstract sketches using language models, emphasizing semantic understanding, prior knowledge, and geometric simplifications for effective yet recognizable abstraction at varied levels.

In *geometric abstraction*, recent research explores diverse techniques for capturing essential geometric elements and structures, including vector image representation [Hirschorn et al. 2024], salient region detection [Cheng et al. 2013], procedural drawing generation using evolutionary algorithms [Tian and Ha 2022], and assembling images from simple parametric primitives [Chen et al. 2023]. While image abstraction typically involves transforming the image into a more abstract or stylized representation, image simplification is typically an essential step in the abstraction process, where unnecessary details are removed to simplify the image before further abstraction techniques are applied. Our work presents a progressive semantic-aware simplification that guides a layered vectorization process, thereby advancing the state-of-the-art (see Figure 11).

## 3 OVERVIEW

Our framework consists of two modules that work sequentially to achieve layered vectorization. One module is *Progressive Image Simplification* that employs Score Distillation Sampling [Poole et al. 2022] combined with semantic segmentation to generate a sequence of images with varying levels of semantic simplicity (see the first row in Figure 1). The other module *Layered Vectorization* uses that series of simplified images as guidance and generates vectors layer by layer, from coarse to fine level of detail (see the second to fourth rows in Figure 1).

Figure 3 illustrates the vector optimization per simplified level. Taking the simplified image at the current level as input, we compute its differences from images from the previous levels to estimate where additional primitives should be best added. This process involves examining differences at two levels: the semantic segmentation level and the pixel level. At the semantic segmentation level, vector primitives are initialized where the segmentation differences are detected, referred to as *structure-wise vector primitives*. At the pixel level, primitives can be optionally initialized (noted as *pixel-wise primitives*). This primitive initialization encourages the vector representation to effectively capture both semantic and pictorial information (Section 5.1).

The newly added primitives, together with the primitives from all previous levels, undergo a joint optimization towards two main losses. One is the *Visual Loss*, which considers the visual fitness of the target image at the current level. The other is the *Structural Loss*, which weighs the impact of shape alignment between structure-wise primitives and their corresponding semantic segmentation to ensure that the vector representation accurately maintains the essential structural semantics. As shown on the right part of Figure 3, both losses are designed as image-space losses by leveraging the capabilities of differential rendering [Li et al. 2020]. Specifically, for structural loss, we first organize structure-wise primitives into distinct layers. Then, for each layer, an MSE-based loss is computed between the rendered image of structure-wise primitives and their corresponding segmentation image. The optimization of the vector primitives is achieved by combining the structural loss from all layers together with the visual loss. Further details regarding the loss shall be provided in Section 5.2. Following this process, we progressively add vector primitives from one simplified level to the next. Once all levels are computed, we organize them into groups with containing and contained relationships to facilitate easier manipulation and editing.

## 4 SEMANTIC SIMPLIFICATION

Our layered vectorization technique is progressively directed by a sequence of images semantically simplified from the original image. Current vectorization techniques primarily perform pixel-level analysis of the input image to decide where to add and optimize paths, such as large connected areas identified by color quantification in LIVE [Ma et al. 2022] or clusters via DBSCAN in Optimize & Reduce (O&R) method [Hirschhorn et al. 2024]. Rather than solely analyzing the original image, our approach involves generating a series of simplified images and their semantic segmented masks derived from the original. Figure 4 shows an example of the simplified image sequence generated using our SDS-based method (Section 4.2). As can be seen, the image sequence exhibits varying levels of simplicity, from the original one with many intricate details and textures to a simplified and overall outline on the right.

The intuition behind using simplified images to guide layered vectorization is to prioritize the capture of the overall structure before addressing subtle changes. This approach offers two notable benefits. Firstly, by decomposing the vectorization process into manageable levels, it becomes more tangible and achievable compared to optimizing it as a whole. The incremental improvement from one abstract level to the next is relatively small, allowing for effective optimization at each step. Secondly, the progressive abstraction establishes a coarse-to-fine hierarchy, enabling holistic optimization of delicate paths within the image. This approach becomes particularly advantageous when dealing with shapes that exhibit pixel variations due to occlusion, shadows, or textures yet remain integral components of a larger entity. For example, in the right of Figure 4, the ‘cat’ is abstracted as a shape unit at the most simplified level, while pixel-based methods such as LIVE or O&R would represent the cat with fragmented shapes and fail to capture the entire cat shape due to the occlusion of the ‘stripped sweater’. Our method favors that these paths are retrieved as complete entities, enhancing the overall editability and preserving the intended structure of the figure.

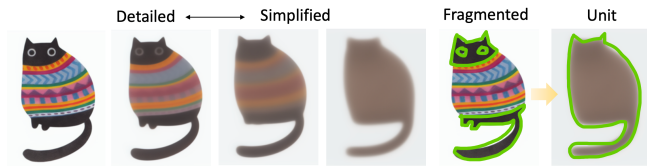


Fig. 4. Layered simplified images: (left) a sequence of simplified images generated with our SDS method, with the original image on the leftmost as input. (right) instead of being represented by individual parts (highlighted in green), cat shape can be captured by a single continuous path with our semantic simplification, on the right.

### 4.1 Pixel-based Simplification

Pixel-based simplification techniques, such as Superpixel [Achanta et al. 2012] and Gaussian low-pass filter, can serve as baseline choices for this purpose. By varying Gaussian kernels with radius from small to large, a sequence of images can be generated by reducing image noise and detail. By changing the number of superpixels, images

can be simplified by various numbers of pixel groups that share common characteristics. Pixel-level simplification methods operate by manipulating the intensity values of individual pixels and their surrounding pixels. While these techniques can effectively reduce the complexity of an image, they do not consider the semantics of the objects present in the image. Consequently, as exemplified in Figure 5, when these methods are applied to high-level abstract, they may inadvertently blur or blend adjacent objects, which introduces significant problems in the contour of semantic segmentation, such as the leakage and inaccurate boundaries of the ‘head of the bird’.

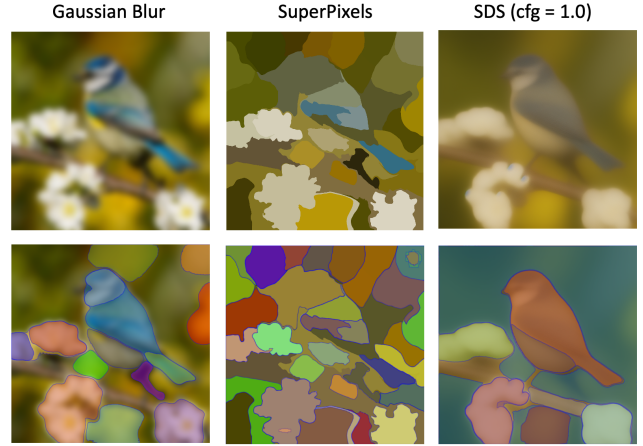


Fig. 5. Compared to pixel-based simplification techniques, e.g., Gaussian blur and SuperPixels, our SDS simplification can maintain the semantics of objects well. With SDS, the boundaries of semantic segmentation are effectively smoothed while still retaining important geometric features, such as the distinct shape of the ‘bird’s mouth’. Note that the top row displays simplified images, while the bottom row shows the corresponding semantic segmentation.

### 4.2 Simplification with SDS

In our work, we introduce a novel semantic simplification technique that makes use of the *Feature-averaged Effect* in Score Distillation Sampling (SDS) [Poole et al. 2022]. As shown in the right column of Figure 5, our SDS-based simplification approach effectively reduces intricate details, such as the feather texture of the bird and the background, while preserving fundamental features, such as a rough silhouette depiction of the bird.

As investigated by Liang et al. [2023], the feature-average effect of SDS can be explained by rewriting the gradient of SDS loss as:

$$\nabla_{\theta} \mathcal{L}_{\text{SDS}}(\theta) = \mathbb{E}_{t, \epsilon} \left[ \frac{\omega(t)}{\gamma(t)} (x_0 - \hat{x}_0^t) \frac{\partial g(\theta)}{\partial \theta} \right], \quad (1)$$

where  $g$  is the differentiable generator that transforms parameters  $\theta$  to create an image  $x = g(\theta)$ , e.g.,  $g$  is a NeRF volume renderer in the original SDS work [Poole et al. 2022]. In our work, we take  $g$  as a generator that renders a single image [Hertz et al. 2023]. Therefore,  $\theta$  are the image pixels. SDS drives the input image  $x_0$  towards the  $\hat{x}_0^t$ , which is averaged from the images with inconsistent features predicted by the diffusion model DDPM [Ho et al. 2020]. The

diffusion model first perturbs  $x_0$  to  $x_t$  with random noises. However, DDPM is overly sensitive to its input, where minor fluctuations in  $x_t$  would change the details of the predicted images. A smoothed image without individual details is achieved by averaging images with local feature-inconsistent.

We have adjusted the Guidance Scale parameter in Classifier-free Guidance (CFG) [Ho and Salimans 2022] to introduce greater variation in the generated images. Specifically, we have reduced the value of the Guidance Scale from its usual value of 7.5 to 1.0. This modification enables the diffusion model to exhibit more creativity and deviate less strictly from the given text prompt.

By different numbers of SDS iterations, a sequence of  $N$  images at different simplified levels can be generated. In our work,  $N$  is set to five, i.e., the origin image and four simplified images sampled every 20 steps throughout 80 SDS iterations. As shown in Figure 5, the SDS method simplifies the image at a very abstract level while effectively maintaining the overall shape of the ‘bird’ and ‘flowers’. It is important to note that although the resulting images appear blurred, they still allow for effective semantic segmentation. Moreover, the boundaries of detected objects are smoothed and compatible with vector-based graphics.

## 5 LAYERED VECTORIZATION

With the sequence of simplified images, layers of vectors are progressively added and optimized from the simplest to the most detailed. Below, we introduce the key components of this part.

### 5.1 Primitive Initialization

During the optimization process of the  $N^{th}$  level ( $N$  valued from small to large, corresponding to the simple to the detailed), vector primitives are strategically initialized at locations where prominent differences are detected from the current image to the previous ones. We primarily consider the differences in semantics, i.e., based on the segmentation difference, and take the pixel-level difference as an additional complementary to the detailed visual effects.

To add structure-wise primitives, semantic segmentation is first applied in the  $N^{th}$  simplified image to categorize pixels into meaning regions, which we refer to as *masks*. Subsequently, the masks from the  $N^{th}$  are compared to the existing masks of the  $N - 1$  levels (as shown in the left of Figure 6 (a)). Only the new masks that were not present in the preceding  $N - 1$  levels are added. If a mask from the current level exhibits a high degree of overlap with existing masks, determined using the Jaccard similarity coefficient [Jaccard 1901], we refrain from adding it, as it likely represents the same semantic object. Once the masks are identified and added, we initialize vector primitives for each one. We use the Douglas-Peucker simplified representation of the masks as the initial shape [Douglas and Peucker 1973]. To delicately capture the complex shapes at this stage, a closed shape composed of eight cubic Bézier curves is used as the basic vector primitive.

To add pixel-wise primitives, we compute the pixel-level difference between the  $N^{th}$  simplicity level and the previous level ( $N - 1$ )<sup>th</sup>. A connected component labeling algorithm is applied over pixels in the  $N^{th}$  simplified image to connect pixels into regions with a maximum difference threshold  $C_{diff}$ . As shown in

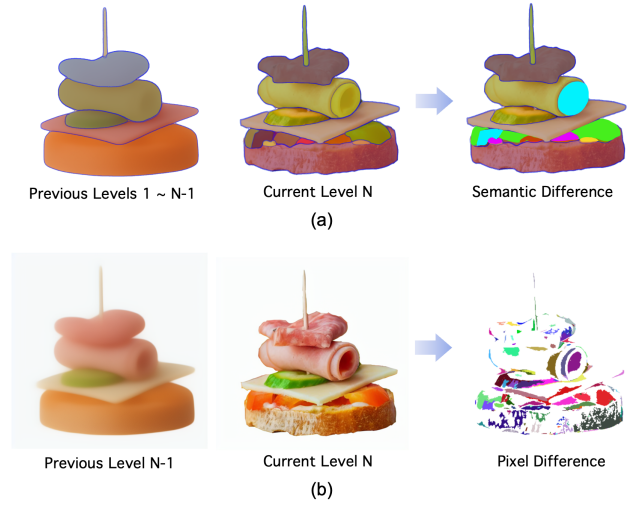


Fig. 6. Path initialization: (a) structure-wise primitives are initialized where differences are identified between semantic segmentation of the current image and previous ones. (b) pixel-wise primitives are initialized around significant pixel-level differences between the current image to its previous one.

Figure 6(b), the pixel-level difference is quite intricate, exhibiting unpredictable or irregular patterns. This suggests that it is challenging to construct a compact vector structure using purely pixel-level analysis, such as the method used in LIVE [Ma et al. 2022]. In our work, we control the complexity of vector representation by a parameter  $P_{num}$ , the number of pixel-level primitives to be added per level. Also, to restrain the complexity, we employ a closed shape of four cubic Bézier curves as the fundamental pixel-wise primitive, which is more straightforward than the structure-wise primitive.

### 5.2 Loss Function

The loss function comprises two main components: the *structural loss*, which measures the alignment of structure-wise primitives to the segmentation across layers, and the *visual loss*, which assesses the visual fitness of all primitives to the simplified image at the current level.

**Structural Loss.** The structural loss  $\mathcal{L}_{structure}$  is computed as the sum of MSE loss over the layers  $M$ . For each layer  $j$ , the structural loss is calculated as the MSE between the rendering of structure-wise primitives at that layer  $I_{layer_j}$  and their corresponding segmentation image  $I_{segment_j}$ . This function concentrates on optimizing shape rather than colors or any other non-spatial visual appearance. Therefore, we assign the same random color to each pair of structure-wise primitives and their corresponding segmentations. With the  $MSE_j$  per layer, the structural loss is defined as:

$$\mathcal{L}_{structure} = \sum_{j=1}^M MSE(I_{layer_j}, I_{segment_j}). \quad (2)$$

**Visual Loss.** The visual loss  $\mathcal{L}_{visual}$  is used to measure the discrepancy between the image rendered from all primitives, denoted as  $I_{render}$ , and the target image at the current simplicity level, denoted as  $I_{target}$ . The visual loss is calculated using the simple MSE method. Mathematically, this can be expressed as:

$$\mathcal{L}_{visual} = \text{MSE}(I_{render}, I_{target}). \quad (3)$$

**Primitive Length Loss.** We introduce a simple loss function  $\mathcal{L}_{length}$  based on the length of the path to ensure the primitive quality. Mathematically, this can be expressed as:

$$\mathcal{L}_{length} = \text{ReLU}(L - L_{\min}), \quad (4)$$

where  $L$  is the length of cubic Bézier curves, and  $L_{\min}$  is set to the minimum length (5 units in our work). By incorporating this loss term into optimization, this approach helps optimize overall path quality by discouraging unnecessarily long paths and promoting the use of more direct and economical routes.

With the above, the loss function is a joint one, as follows:

$$\mathcal{L}_{total} = \mathcal{L}_{visual} + \beta \mathcal{L}_{structure} + \delta \mathcal{L}_{length}, \quad (5)$$

where the parameters  $\beta$  and  $\delta$  are used to balance the contribution of each loss component to the total loss. This joint loss function allows the model to optimize for visual accuracy, structural integrity, and curve length simultaneously.

## 6 IMPLEMENTATION DETAILS

We implemented this method using PyTorch with the Adam optimizer. By default, a sequence of five simplified images (including the original input image) is generated at intervals of 20 SDS iterations. The learning rates for optimizing primitive points and their colors are set to 1.0 and 0.01, respectively. In Equation 5 of the joint loss function, the  $\beta$  is set to 1, and  $\delta$  is set to 0.1. During the optimization (Figure 3), we performed the optimization through 100 iterations at each level of simplicity except the last level. For the last level of simplicity, we conducted 500 iterations to achieve optimal results. At the end of each iteration, primitives shorter than 25 units are removed. Pixel-wise primitives are initialized as circular shapes with a radius of 5 units, following the approach used in LIVE [Ma et al. 2022]. All examples and experiments in this paper were conducted on a system running Ubuntu 20.04.6 LTS, equipped with an Intel Xeon Gold 5320 CPU operating at 2.20 GHz and four NVIDIA A40 GPUs. Each GPU features 48 GB of GDDR6 memory with ECC.

## 7 RESULTS

In this section, we present the results of our method and some applications in vector editing and design.

**Layered Representation.** In Figure 7, we show the vectorization and its layered structure generated from the image shown on the left top. As can be seen, semantic objects can be distinctly represented using a set of vector primitives from back to front (see on the left). For example, for the ‘pink truck’, our method creates a vector primitive to represent the entire truck, over which primitives with secondary semantics, such as the ‘cab’ and ‘cargo area’, are layered separately.



Fig. 7. An example of layered representation: vectorized from the input image ‘transportation’ on the left-top, our method can generate distinct vectors by semantics.

Figure 8 presents the layer structure of four more examples. For each example, the first four columns display the structure-wise primitives across four layers. The rightmost column presents the final vectorization result, including the pixel-wise primitives. As illustrated, structure-wise primitives are progressively generated from back to front and from large to small detailed shapes. With structure-wise primitives serving as the backbone, pixel-wise primitives are well contained within them. Figure 10 provides more examples of the layering.

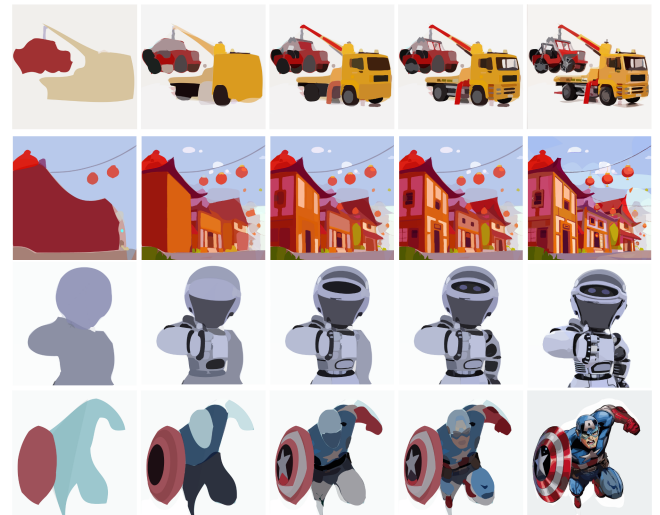


Fig. 8. Sequences of five vectorized layers: each row displays the back-to-front layers consisting of structure-wise primitives. The rightmost column presents the final result, incorporating the addition of pixel-wise primitives.

**Vector Editing.** Figure 9 shows an example of applying our method together with the state-of-the-art methods, i.e., O&R [Hirschorn

et al. 2024] and LIVE [Ma et al. 2022] to an image of ‘ice cream’. As demonstrated, the visual appeal of vectors generated by our method is noticeably superior to that produced by O&R and is comparable to, if not better than, that by LIVE. From the perspective of structure, our method generates much more manageable and compact vectors, such as the ‘ice cream ball’ and ‘bowl’ organized in a grouping structure. The layering and grouping structure that we constructed in our vectorization process significantly enhances the ease of vector editing. For instance, the task of recoloring semantic parts within the vector can be accomplished with just a few operation steps. Figure 9(d) provides a practical demonstration of this utility. A semantic group of visual primitives can be easily selected by taking the group segmentation at a certain layer as the selector. For example, we can select all vector primitives related to the ‘pink ice cream ball’ with a single click on the corresponding structure-wise primitive. With the selected groups, subsequently, we can effectively change the color of the semantic objects by adjusting the hues of all selected paths by a specific offset while maintaining the saturation and brightness constant. This process results in an organically transposed style, yielding an ice cream ball with a fresh color yet preserving its original texture and lighting.

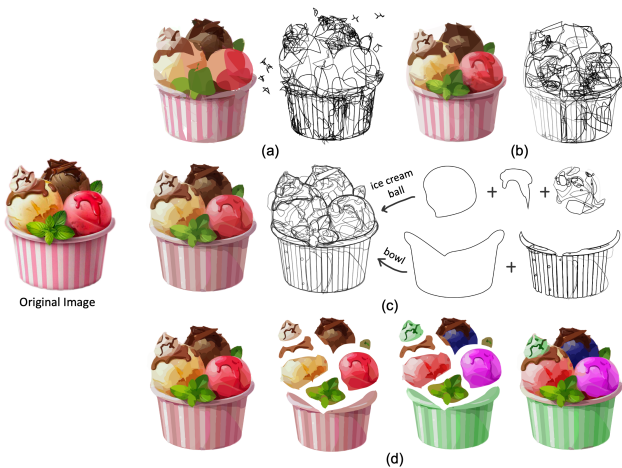


Fig. 9. Vectorization and recoloring of an ‘ice cream’ image: compared to vectors generated by (a) O&R [Hirschorn et al. 2024] and (b) LIVE [Ma et al. 2022], (c) our method generates a more structured vector representation. Note the hierarchies of ‘ball’ and ‘bowl’. (d) With our layered vector representation, the vectors facilitate altering colors in a few steps: from left to right, the original image, selected groups of primitives by clicking the back primitive container, and change the color style by shifting the hue channel of a fixed offset.

## 8 EXPERIMENTS

In this section, we present a quantitative analysis conducted among LIVE, O&R, and our technique from the perspective of visual quality, time consumption, and representation compactness.

In Figure 11, we show examples of the three vectorization techniques. To make the comparison fair, we use 256 visual primitives for all three methods. For O&R [Hirschorn et al. 2024], we used an optimize and reduce process of 1024, 768, 512, 384, and 256 primitives.

For our method, we employed a simple strategy to precisely limit the number of visual primitives to 256. Specifically, we optimized the structure-wise primitives for  $N$  levels of simplicity first, after which we added and optimized pixel-wise primitives to ensure the total primitive count reached 256. Overall, our method demonstrates the improvements over existing methods.

*Visual Fidelity.* In this section, we examined the visual rendering fidelity of the generated vectors, specifically how closely they resemble the original input image. To quantify this, we calculated the mean squared error (MSE) between the rendering image of vectors and the original image. Table 2 shows the result for the ten examples in Figure 11. Except for the ‘animals’, our method generates vectors with higher visual quality than the other two baseline methods in other examples. For instance, in the ‘hamburger’ example, our method accurately renders the ‘sesame on the bread’, whereas the other two methods fail to do so. Similarly, in the ‘boat’ example, our method recovers the ‘reflection on water with letters’, which the other methods do not capture effectively.

*Time Consumption.* We measured the time required by the three techniques to generate the ten examples in Figure 11. LIVE exhibited the highest execution time, averaging 37 minutes per image. Conversely, O&R demonstrated the lowest time consumption, requiring approximately 14 minutes to generate image vectors. Our proposed method achieved a balance between the two, with an average processing time of 16 minutes per image. Details regarding the execution time for each technique are provided in Table 1.

	LIVE	O&R	Ours
hamburger	2111	805	888
fish	2229	886	1046
peak	2456	918	1071
animals	2199	958	1011
wolf	2385	835	1025
butterfly	2447	908	1044
fisherman	2142	883	967
boat	2390	907	919
bike	2289	869	1042
landscape	2125	831	1064
Average (s)	2277.3	880.0	1007.7
Std.	134.5	46.3	62.6

Table 1. Time cost of ten examples (s) in Figure 11.

*Vector Representation.* We introduce the metric *Vector Compactness (VeC)* to assess how well the primitives are grouped and contained. Given a semantic mask (e.g., the area of pixels segmented as ‘butterfly’), VeC is defined as the ratio between the number of primitives with high containment within the mask (i.e., exceeding 90% area overlap) and the total number of primitives interacting with the mask. We evaluated this metric by sampling four semantic masks from each image example in Figure 11 and computing the average VeC per image. As presented in Table 2, our proposed method maintains significantly higher compactness of primitives compared

Table 2. MSE and vector compactness of ten examples in Figure 11: our method outperforms LIVE and O&R in terms of both visual and structural reconstruction quality.

	MSE			Vector Compact (%)		
	LIVE	O&R	Ours	LIVE	O&R	Ours
hamburger	0.0047	0.0082	0.0011	18.0	11.4	56.7
fish	0.0104	0.0124	0.0094	24.1	18.2	48.5
peak	0.0045	0.0033	0.0018	11.7	9.9	35.2
animals	0.0038	0.0055	0.0040	8.3	9.4	43.8
wolf	0.0017	0.0025	0.0015	22.7	12.1	36.2
butterfly	0.0031	0.0045	0.0025	15.9	19.0	44.5
boat	0.0050	0.0065	0.0036	24.7	19.4	47.7
fisherman	0.0044	0.0047	0.0033	15.2	16.9	42.0
bike	0.0057	0.0078	0.0045	30.4	17.4	49.6
landscape	0.0055	0.0071	0.0050	27.8	12.8	34.5
<b>Average</b>	<b>0.0049</b>	<b>0.0063</b>	<b>0.0037</b>	<b>19.9</b>	<b>14.7</b>	<b>43.9</b>
<b>Std.</b>	<b>0.0023</b>	<b>0.0029</b>	<b>0.0024</b>	<b>7.17</b>	<b>3.89</b>	<b>7.14</b>

to the other two methods, with approximately 43.9%, while only 19.9% and 14.7% for LIVE and O&R, respectively. Furthermore, as visually evident in Figure 11, primitives in LIVE or O&R tend to exhibit scattering and inter-region intersections. In contrast, our method demonstrates superior performance by effectively retaining nearly half of the visual primitives within their designated semantic structures.

## 9 CONCLUSIONS

We have introduced a progressive image vectorization technique that provides a compact representation of geometric primitives through layered vectorization. Our method prioritizes capturing the overall structure before adding layers with finer details by utilizing a series of simplified images to guide this process. This approach offers two main advantages. First, it decomposes the vectorization process into manageable portions, enhancing optimization efficiency at each step and enabling comprehensive refinement of complex paths. Second, it establishes a coarse-to-fine hierarchy, where coarse levels capture larger structural elements and fine levels address smaller, detailed components. Overall, as demonstrated, our method produces a vectorized representation that is significantly more user-friendly and effective than those produced by current state-of-the-art techniques, greatly enhancing usability for further editing and modification.

In this paper, we refer to and claim that our method is an image simplification technique rather than an image abstraction. While the two concepts share similarities, they diverge in their primary objectives. Image abstraction aims to represent images in a stylized manner while retaining essential characteristics, whereas image simplification prioritizes reducing complexity in a hierarchical manner. Our approach for abstraction is applying a semantic-aware simplification, but it does not include stylization aspects. Our primary goal was to generate compact and manageable vectorized representations. Future endeavors will explore the integration of stylization aspects into our framework.

## REFERENCES

- Radhakrishna Achanta, Appu Shaji, Kevin Smith, Aurelien Lucchi, Pascal Fua, and Sabine Süsstrunk. 2012. SLIC superpixels compared to state-of-the-art superpixel methods. *IEEE transactions on pattern analysis and machine intelligence* 34, 11 (2012), 2274–2282.
- Radhakrishna Achanta and Sabine Susstrunk. 2017. Superpixels and polygons using simple non-iterative clustering. In *Proceedings of the IEEE conference on computer vision and pattern recognition*. 4651–4660.
- Alexandre Carlier, Martin Danelljan, Alexandre Alahi, and Radu Timofte. 2020. Deepsvg: A hierarchical generative network for vector graphics animation. *Advances in Neural Information Processing Systems* 33 (2020), 16351–16361.
- Ye Chen, Bingbing Ni, Xuanhong Chen, and Zhangli Hu. 2023. Editable Image Geometric Abstraction via Neural Primitive Assembly. In *Proceedings of the IEEE/CVF International Conference on Computer Vision (ICCV)*. 23514–23523.
- Ming-Ming Cheng, Jonathan Warrell, Wen-Yan Lin, Shuai Zheng, Vibhav Vineet, and Nigel Crook. 2013. Efficient Saliency Region Detection with Soft Image Abstraction. In *Proceedings of the IEEE International Conference on Computer Vision (ICCV)*.
- Edoardo Alberto Dominici, Nico Schertler, Jonathan Griffin, Shayan Hoshary, Leonid Sigal, and Alla Sheffer. 2020. PolyFit: perception-aligned vectorization of raster clip-art via intermediate polygonal fitting. *ACM Trans. Graph.* 39, 4, Article 77 (aug 2020), 16 pages. <https://doi.org/10.1145/3386569.3392401>
- David H Douglas and Thomas K Peucker. 1973. Algorithms for the reduction of the number of points required to represent a digitized line or its caricature. *Cartographica: the international journal for geographic information and geovisualization* 10, 2 (1973), 112–122.
- Zheng-Jun Du, Liang-Fu Kang, Jianchao Tan, Yotam Gingold, and Kun Xu. 2023. Image vectorization and editing via linear gradient layer decomposition. *ACM Transactions on Graphics (TOG)* 42, 4 (2023), 1–13.
- Maria Dziuaba, Ivan Jarsky, Valeria Efimova, and Andrey Filchenkov. 2023. Image Vectorization: a Review. arXiv:2306.06441 [cs.CV]
- Vage Egiuzarian, Oleg Voynov, Alexey Artemov, Denis Volkhonskiy, Aleksandr Safin, Maria Taktasheva, Denis Zorin, and Evgeny Burnaev. 2020. Deep Vectorization of Technical Drawings. In *Computer Vision – ECCV 2020: 16th European Conference, Glasgow, UK, August 23–28, 2020, Proceedings, Part XIII* (<conf-loc content-type="InPerson">Glasgow, United Kingdom-</conf-loc->). Springer-Verlag, Berlin, Heidelberg, 582–598. [https://doi.org/10.1007/978-3-030-58601-0\\_35](https://doi.org/10.1007/978-3-030-58601-0_35)
- Jean-Dominique Favreau, Florent Lafarge, and Adrien Bousseau. 2017. Photo2clipart: image abstraction and vectorization using layered linear gradients. *ACM Trans. Graph.* 36, 6, Article 180 (nov 2017), 11 pages. <https://doi.org/10.1145/3130800.3130888>
- Jon Ferraiolo, Fujisawa Jun, and Dean Jackson. 2000. *Scalable vector graphics (SVG) 1.0 specification*. iuniverse Bloomington.
- Kevin Frans, Lisa Soros, and Olaf Witkowski. 2022. CLIPDraw: Exploring Text-to-Drawing Synthesis through Language-Image Encoders. In *Advances in Neural Information Processing Systems*, S. Koyejo, S. Mohamed, A. Agarwal, D. Belgrave, K. Cho, and A. Oh (Eds.), Vol. 35. Curran Associates, Inc., 5207–5218. [https://proceedings.neurips.cc/paper\\_files/paper/2022/file/21f76686538a5f06dc431efea5f475f5-Paper-Confidence.pdf](https://proceedings.neurips.cc/paper_files/paper/2022/file/21f76686538a5f06dc431efea5f475f5-Paper-Confidence.pdf)
- Amir Hertz, Kfir Aberman, and Daniel Cohen-Or. 2023. Delta denoising score. In *Proceedings of the IEEE/CVF International Conference on Computer Vision*. 2328–2337.
- Or Hirschorn, Amir Jevnisek, and Shai Avidan. 2024. Optimize & Reduce: A Top-Down Approach for Image Vectorization. In *Proceedings of the AAAI Conference on Artificial Intelligence*, Vol. 38. 2148–2156.
- Jonathan Ho, Ajay Jain, and Pieter Abbeel. 2020. Denoising diffusion probabilistic models. *Advances in neural information processing systems* 33 (2020), 6840–6851.
- Jonathan Ho and Tim Salimans. 2022. Classifier-free diffusion guidance. *arXiv preprint arXiv:2207.12598* (2022).
- Shayan Hoshary, Edoardo Alberto Dominici, Alla Sheffer, Nathan Carr, Zhaowen Wang, Duygu Ceylan, and I-Chao Shen. 2018. Perception-driven semi-structured boundary vectorization. *ACM Trans. Graph.* 37, 4, Article 118 (jul 2018), 14 pages. <https://doi.org/10.1145/3197517.3201312>
- Paul Jaccard. 1901. Étude comparative de la distribution florale dans une portion des Alpes et des Jura. *Bull Soc Vaudoise Sci Nat* 37 (1901), 547–579.
- Ajay Jain, Amber Xie, and Pieter Abbeel. 2023. Vectorfusion: Text-to-svg by abstracting pixel-based diffusion models. In *Proceedings of the IEEE/CVF Conference on Computer Vision and Pattern Recognition*. 1911–1920.
- Alexander Kirillov, Eric Mintun, Nikhila Ravi, Hanzi Mao, Chloe Rolland, Laura Gustafson, Tete Xiao, Spencer Whitehead, Alexander C Berg, Wan-Yen Lo, et al. 2023. Segment anything. In *Proceedings of the IEEE/CVF International Conference on Computer Vision*. 4015–4026.
- Subhadeep Koley, Ayan Kumar Bhunia, Aneeshan Sain, Pinaki Nath Chowdhury, Tao Xiang, and Yi-Zhe Song. 2024. How to Handle Sketch-Abstraction in Sketch-Based Image Retrieval? arXiv:2403.07203 [cs.CV]
- Gregory Lecot and Bruno Levy. 2006. Ardeco: Automatic region detection and conversion. In *17th Eurographics Symposium on Rendering-EGSR'06*. 349–360.



- Tzu-Mao Li, Michal Lukáč, Michaël Gharbi, and Jonathan Ragan-Kelley. 2020. Differentiable vector graphics rasterization for editing and learning. *ACM Trans. Graph.* 39, 6, Article 193 (nov 2020), 15 pages. <https://doi.org/10.1145/3414685.3417871>
- Yixun Liang, Xin Yang, Jiantao Lin, Haodong Li, Xiaogang Xu, and Yingcong Chen. 2023. Luciddreamer: Towards high-fidelity text-to-3d generation via interval score matching. *arXiv preprint arXiv:2311.11284* (2023).
- Zicheng Liao, Hugues Hoppe, David Forsyth, and Yizhou Yu. 2012. A subdivision-based representation for vector image editing. *IEEE transactions on visualization and computer graphics* 18, 11 (2012), 1858–1867.
- Raphael Gontijo Lopes, David Ha, Douglas Eck, and Jonathon Shlens. 2019. A learned representation for scalable vector graphics. In *Proceedings of the IEEE/CVF International Conference on Computer Vision*. 7930–7939.
- Xu Ma, Yuqian Zhou, Xingqian Xu, Bin Sun, Valerii Filev, Nikita Orlov, Yun Fu, and Humphrey Shi. 2022. Towards layer-wise image vectorization. In *Proceedings of the IEEE/CVF Conference on Computer Vision and Pattern Recognition*. 16293–16302. <https://doi.org/10.1109/CVPR52688.2022.01583>
- Ben Poole, Ajay Jain, Jonathan T Barron, and Ben Mildenhall. 2022. Dreamfusion: Text-to-3d using 2d diffusion. *arXiv preprint arXiv:2209.14988* (2022).
- Pradyumna Reddy, Michael Gharbi, Michal Lukac, and Niloy J Mitra. 2021. Im2vec: Synthesizing vector graphics without vector supervision. In *Proceedings of the IEEE/CVF Conference on Computer Vision and Pattern Recognition*. 7342–7351.
- Pradyumna Reddy, Paul Guerrero, Matt Fisher, Wilmot Li, and Niloy J Mitra. 2020. Discovering pattern structure using differentiable compositing. *ACM Transactions on Graphics (TOG)* 39, 6 (2020), 1–15.
- Juan A Rodriguez, Shubham Agarwal, Issam H Laradji, Pau Rodriguez, David Vazquez, Christopher Pal, and Marco Pedersoli. 2023. StarVector: Generating Scalable Vector Graphics Code from Images. *arXiv preprint arXiv:2312.11556* (2023).
- I-Chao Shen and Bing-Yu Chen. 2022. ClipGen: A Deep Generative Model for Clipart Vectorization and Synthesis. *IEEE Transactions on Visualization and Computer Graphics* 28, 12 (dec 2022), 4211–4224. <https://doi.org/10.1109/TVCG.2021.3084944>
- Jian Sun, Lin Liang, Fang Wen, and Heung-Yeung Shum. 2007. Image vectorization using optimized gradient meshes. *ACM Trans. Graph.* 26, 3 (jul 2007), 11–es. <https://doi.org/10.1145/1276377.1276391>
- Xingze Tian and Tobias Günther. 2024. A Survey of Smooth Vector Graphics: Recent Advances in Representation, Creation, Rasterization, and Image Vectorization. *IEEE Transactions on Visualization and Computer Graphics* 30, 3 (2024), 1652–1671. <https://doi.org/10.1109/TVCG.2022.3220575>
- Yingtao Tian and David Ha. 2022. Modern Evolution Strategies for Creativity: Fitting Concrete Images and Abstract Concepts. In *Artificial Intelligence in Music, Sound, Art and Design: 11th International Conference, EvoMUSART 2022, Held as Part of EvoStar 2022, Madrid, Spain, April 20–22, 2022, Proceedings* (Madrid, Spain). Springer-Verlag, Berlin, Heidelberg, 275–291. [https://doi.org/10.1007/978-3-031-03789-4\\_18](https://doi.org/10.1007/978-3-031-03789-4_18)
- Y. Vinker, Y. Alaluf, D. Cohen-Or, and A. Shamir. 2023. CLIPascene: Scene Sketching with Different Types and Levels of Abstraction. In *2023 IEEE/CVF International Conference on Computer Vision (ICCV)*. IEEE Computer Society, Los Alamitos, CA, USA, 4123–4133. <https://doi.org/10.1109/ICCV51070.2023.00383>
- Yael Vinker, Ehsan Pajouheshgar, Jessica Y Bo, Roman Christian Bachmann, Amit Haim Bermano, Daniel Cohen-Or, Amir Zamir, and Ariel Shamir. 2022. Clipasso: Semantically-aware object sketching. *ACM Transactions on Graphics (TOG)* 41, 4 (2022), 1–11.
- Tian Xia, Binbin Liao, and Yizhou Yu. 2009. Patch-based image vectorization with automatic curvilinear feature alignment. *ACM Transactions on Graphics (TOG)* 28, 5 (2009), 1–10.
- Guofu Xie, Xin Sun, Xin Tong, and Derek Nowrouzezahrai. 2014. Hierarchical diffusion curves for accurate automatic image vectorization. *ACM Trans. Graph.* 33, 6, Article 230 (nov 2014), 11 pages. <https://doi.org/10.1145/2661229.2661275>



Fig. 10. Gallery of examples generated by our layered vectorization technique: given the input image on the right-most, our method progressively generates layers of vectors, transitioning from coarse to finely detailed representations.  
, Vol. 1, No. 1, Article . Publication date: June 2024.

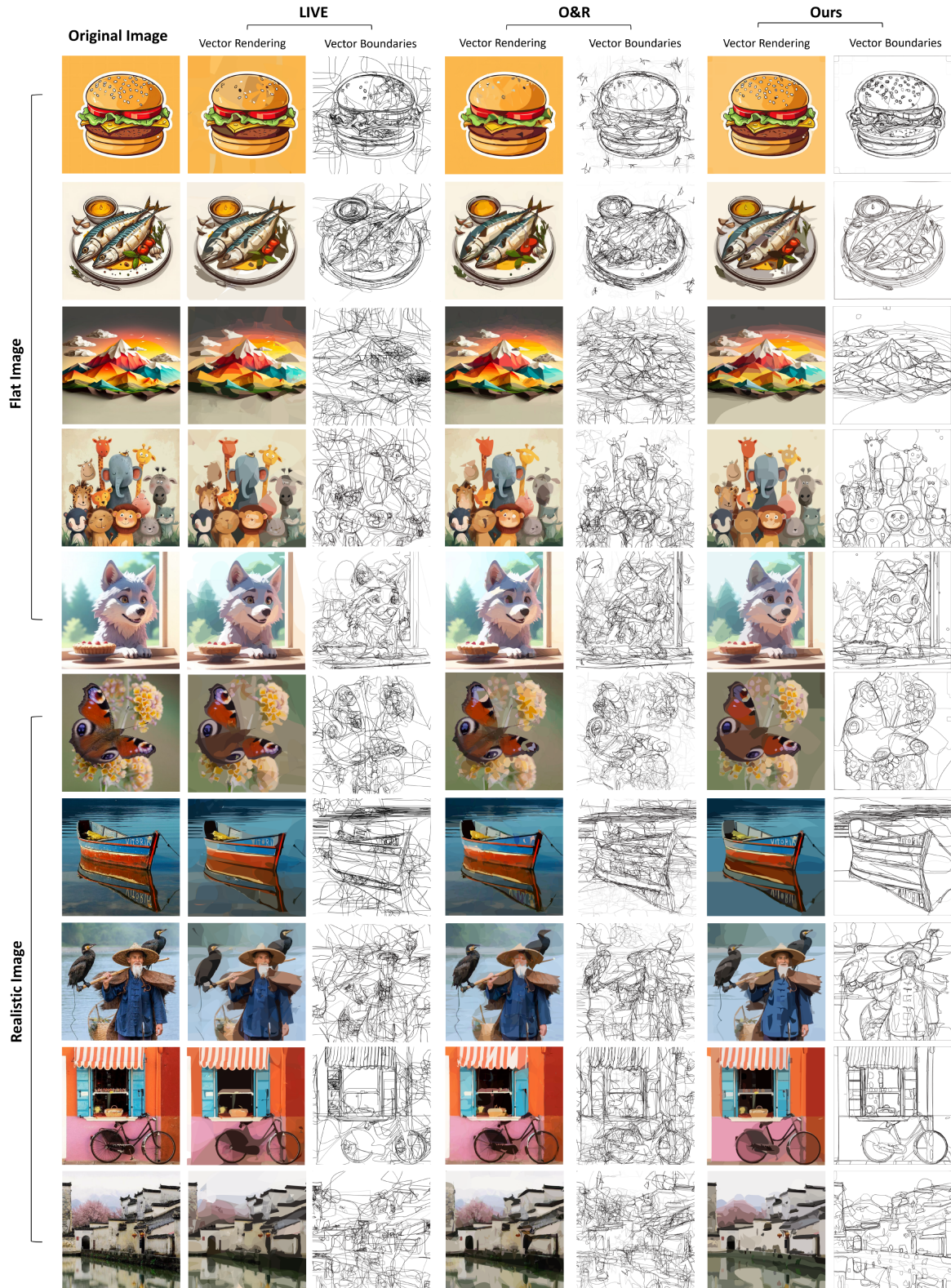


Fig. 11. Gallery of examples generated by three image vectorization techniques, i.e., LIVE [Ma et al. 2022], O&R [Hirschorn et al. 2024] and ours.